Diffusion Dynamics of the Li^+ Ion on a Model Surface of Amorphous Carbon: A Direct Molecular Orbital Dynamics Study

Hiroto Tachikawa* and Akira Shimizu

Division of Materials Chemistry, Graduate School of Engineering, Hokkaido University, Sapporo 060-8628, Japan

Received: March 17, 2005; In Final Form: May 11, 2005

Diffusion processes of the Li^+ ion on a model surface of amorphous carbon ($Li^+C_{96}H_{24}$ system) have been investigated by means of the direct molecular orbital (MO) dynamics method at the semiempirical AM1 level. The total energy and energy gradient on the full-dimensional AM1 potential energy surface were calculated at each time step in the dynamics calculation. The optimized structure, where Li^+ is located in the center of the cluster, was used as the initial structure at time zero. The dynamics calculation was carried out in the temperature range 100−1000 K. The calculations showed that the Li^+ ion vibrates around the equilibrium point below 200 K, while the Li^+ ion moves on the surface above 250 K. At intermediate temperatures (300 K < T < 400 K), the ion moves on the surface and falls in the edge regions of the cluster. At higher temperatures (600 K < T), the Li^+ ion transfers freely on the surface and edge regions. The diffusion pathway of the Li^+ ion was discussed on the basis of theoretical results.

1. Introduction

Graphite is one of the typical compounds possessing a layer structure where various kinds of chemical species can be intercalated into the layers.[1−7] This character has been applied to the anode material as a lithium secondary battery with the excellent performance for the high electromotive force and high energy density.[3] The theoretical maximum capacity for graphitic materials (LiC_6) is 372 mAh/g.[8] In actuality, the capacity is strongly dependent on the structure of carbon materials. Recent investigation has shown that amorphous carbon materials can achieve remarkably high capacities (500−1100 mAh/g).[9,10] This is due to the fact that the amorphous carbon is composed of small carbon clusters without a layer structure and has a high density storage of Li ions in cavity or in edge site (Li_xC_6, x > 1.0).

The reaction in the lithium battery is schematically expressed by

$$Li_nMO_2 + CM \underset{\text{discharge}}{\overset{\text{charge}}{\longleftrightarrow}} Li_{n-1}MO_2 + Li_nCM$$

where MO_2 is metal oxides such as CoO_2 and V_2O_5 and CM means carbon material. The lithium compound ($LiMO_2$) is usually used as a cathode electrode, and the carbon material (without lithium) is used for an anode electrode. The lithium ion (Li^+) is dissolved from cathode to solution in the case of the charge. The Li^+ ion penetrates and diffuses on the carbon cluster of the amorphous carbon.

The elucidation of the diffusion processes of the Li^+ ion on the amorphous carbon is one of the important themes in the development of higher performance lithium secondary batteries. However, the dynamics feature of the diffusion of Li^+ is scarcely known due to the lack of a theoretical method to treat the diffusion dynamics at the quantum mechanical level of theory. Recently, we have developed a dynamics method to calculate the trajectory on the full-dimensional potential energy surface obtained by ab initio and semiempirical molecular orbital (MO) methods.[10−13] This method has been applied to chemical reactions, dynamics of molecular clusters, and diffusions of atoms and ions in materials.[10−13]

In the present paper, diffusion processes of the Li^+ ion on the model cluster of amorphous carbon are investigated by means of the direct MO method. As a model of amorphous carbon, the $C_{96}H_{24}$ cluster model is employed. In particular, we focus our attention on the diffusion path of the Li^+ ion on the amorphous carbon because this is strongly related to the ion conductivity in the amorphous carbon.

The interactions between Li^+ and a graphite surface have been investigated theoretically by several groups using lithium−small carbon cluster models. Marquez et al. calculated the interaction between Li^+ and the hydrogen terminated cluster model ($C_{32}H_{18}$) using the density functional theory (DFT) method and indicated that the Li^+ ion is preferentially bound outside of the cluster model (i.e, the edge site).[14] On the basis of semiempirical MO calculations using a C_{96} planer carbon cluster and Li^+, Nakadaira et al. suggested that the edge site is more stable than that of the bulk.[15] The tight binding calculations showed that a flat band composed of side edge carbon atoms is located near the Fermi level.[16] Ab initio calculations for the interaction of the lithium *atom* with graphite model clusters indicated that charge transfer from the Li atom to the graphite cluster is important in the large cluster size.[17,18]

Lunell et al. calculated the diffusion barriers of Li and Na atoms in the model of TiO_2 film using ab initio and INDO calculations. The barrier for Li diffusion is slightly lower than that of Na diffusion.[19] Yamabe and co-workers investigated the interaction of the Li atom with polycyclic hydrocarbon molecules (pyrene, anthracene, and phenanthrene).[20] The binding energies for several sites are calculated using the B3LYP/6-31G(d)//HF/6-31G* level. More recently, Suzuki et al. investigated the storage state of the Li^+ ion with a $C_{54}H_{18}$ cluster using the PM3 method.[21] Thus, the static feature about the

* To whom correspondence should be addressed. E-mail: hiroto@eng.hokudai.ac.jp. Fax: +81-11-706-7897.

10.1021/jp051418s CCC: $30.25
Published on Web 06/16/2005

interaction between Li^+/Li and the graphite cluster model has been extensively studied. However, the information about the dynamics feature of Li^+ on the amorphous carbon surface is still unclear.

To elucidate the mechanism of a lithium battery, many experimental works have been carried out. Jungblut and Hoinkis investigated experimentally the diffusion kinetics of Li on highly oriented pyrolytic graphite (HOPG) at Li dilute concentration and in a temperature range from 1000 to 1300 K using the isotopes ^{7}Li and ^{6}Li. The Li transport in HOPG is strongly anisotropic. The Li diffusion coefficient (D) in the direction of graphite plane is measured to be $D = 7.6 \times 10^{-9}$ m^2/s at 1070 K.[22] From β-nuclear magnetic resonance (β-NMR) measurement,[23] it is observed that the lithium diffuses in the form of an ion in the graphite layer. The diffusivity is dependent upon the intercalation level. Moreover, from the analysis of lattice image and NMR spectra, Sato et al. predicted that the Li atom exists in disordered carbons.[24] In the present work, the diffusion dynamics of the Li^+ ion on a model cluster of amorphous carbon is investigated by means of the direct MO dynamics method.

2. Method

The amorphous carbons have a nonstacking structure and are composed of small-sized carbon clusters.[25,26] Large amounts of lithium atoms are adsorbed on the carbon layer and edge regions.[15,16] Considering these features, we have chosen a cluster composed of $C_{96}H_{24}$ as the model of amorphous carbon throughout. The similar and smaller carbon clusters have been widely used as a good model of amorphous carbon[27] and/or a surface model of graphite.

First, the model cluster ($C_{96}H_{24}$) was fully optimized at the semiempirical MO level (AM1). For the interaction system ($Li^+C_{96}H_{24}$), one Li^+ ion was put on several initial points above the surface of the cluster, and then, the structures of the $Li^+C_{96}H_{24}$ clusters were fully optimized in order to obtain the trapping sites and relative energies between trapping sites.

Diffusion processes of Li^+ on the surface were investigated by means of the direct MO dynamics method. The total energy and energy gradient on the multidimensional potential energy surface of the $Li^+C_{96}H_{24}$ system were calculated at each time step at the AM1 MO level of theory, and then, the classical equation of motion was full-dimensionally solved. Therefore, the charges and electronic states of the Li^+ ion and all carbon and hydrogen atoms are exactly treated within the level of theory by the calculations at each time step. This point is quite different from classical molecular dynamics (MD) calculations where the charges of all atoms and ions are constant during the diffusion. Hence, one can obtain details of the diffusion processes of the lithium ion on amorphous carbon using the direct MO dynamics method.

We carried out the direct MO dynamics calculations under constant temperature conditions. The mean temperature of the system is defined by

$$T = \frac{1}{3kN}\left\langle \sum_i m_i v_i^2 \right\rangle \tag{1}$$

where N is the number of atoms, v_i and m_i are the velocity and mass of the ith atom, and k is Boltzmann's constant. We choose the following 11 simulation temperatures: 100, 200, 250, 300, 400, 500, 600, 700, 750, 900, and 1000 K. The velocities of atoms at the starting point were adjusted to the selected temperature. The momentum vector of Li^+ at time zero was assumed to be zero, meaning that the ion moves by coupling with the phonon mode of the carbon cluster. To keep a constant temperature of the system, the bath relaxation time (τ) was introduced in the calculation.[28] We have chosen $\tau = 0.01$ ps in all trajectory calculations. The equations of motion for n atoms in the system are given by

$$\frac{dQ_j}{dt} = \frac{\partial H}{\partial P_j}$$

$$\frac{\partial P_j}{\partial t} = -\frac{\partial H}{\partial Q_j} = -\frac{\partial U}{\partial Q_j} \tag{2}$$

where $j = 1-3N$; H is a classical Hamiltonian; and Q_j, P_j, and U are the Cartesian coordinate of the jth mode, conjugated momentum, and potential energy of the system. These equations were numerically solved by the Runge−Kutta method. No symmetry restriction was applied to the calculation of the gradients. The time step size was chosen by 0.2 fs, and a total of 10 000 steps were calculated for each dynamics calculation. The drift of the total energy is confirmed to be less than 1×10^{-3}% throughout all steps in the trajectory. The momentum of the center of mass and the angular momentum are assumed to be zero.

Static density functional theory (DFT) calculations and AM1 calculations for the potential energy curves (PECs) along a diffusion path on a carbon cluster were carried out using the Gaussian 03 program package.[29]

3. Results

A. Structures of the Model Cluster of Amorphous Carbon. The structures of the cluster model ($C_{96}H_{24}$) and the Li^+ adsorbed cluster model ($Li^+C_{96}H_{24}$) are fully optimized at the AM1 MO level of theory. The cluster model has nine different trapping sites for the Li^+ ion. These are six and three trapping sites on the surface (denoted by sites A−F) and in the edge of the surface (denoted by sites a, b, and c), respectively. The optimized structure of Li^+ trapped in site A is illustrated in Figure 1. The cluster model without the Li^+ ion is purely planar, while the structure is changed to a convex-lens-like structure after the interaction with the Li^+ ion. The optimized parameters for site A are $r_1 = 2.6591$, $r_2 = 2.6597$ Å, and $\theta = 57.3°$. The Li^+ ion is located at 2.2367 Å higher from the molecular plane of the cluster. The C−C bond lengths for the cluster model without Li^+ are calculated in the range 1.410−1.440 Å around site A, while the bonds are slightly elongated by the interaction with the Li^+ ion; for example, the C−C bond length near the Li^+ ion is changed from 1.4136 to 1.4379 Å. The geometry optimization for site c gives the structure of site D, indicating that the position of site c is unstable in energy.

The relative energies (ΔE) for all trapping sites are given in Table 1. The zero level of ΔE corresponds to the energy of site A. The Li^+ ions trapped in sites A, B, and C have similar energies. Site D is 5.9 kcal/mol lower in energy than site A, which is the most stable site on the surface of the $C_{96}H_{24}$ cluster. The edge sites (a and b) are more stable in energy than the surface sites.

The Mulliken atomic charge of the Li^+ ion is calculated to be +0.734 at site A, indicating that about 30% of the electrons are transferred from the cluster to the Li^+ ion by the interaction. The charges of all carbon atoms are almost neutral in the free cluster model ($C_{96}H_{24}$). By interacting with the Li^+ ion, the charges on both the C_1 and C_1' atoms of the cluster decrease from 0.0 to −0.03. For the other trapping sites (B−F), a similar structural change and decrease of charges on carbon atoms are

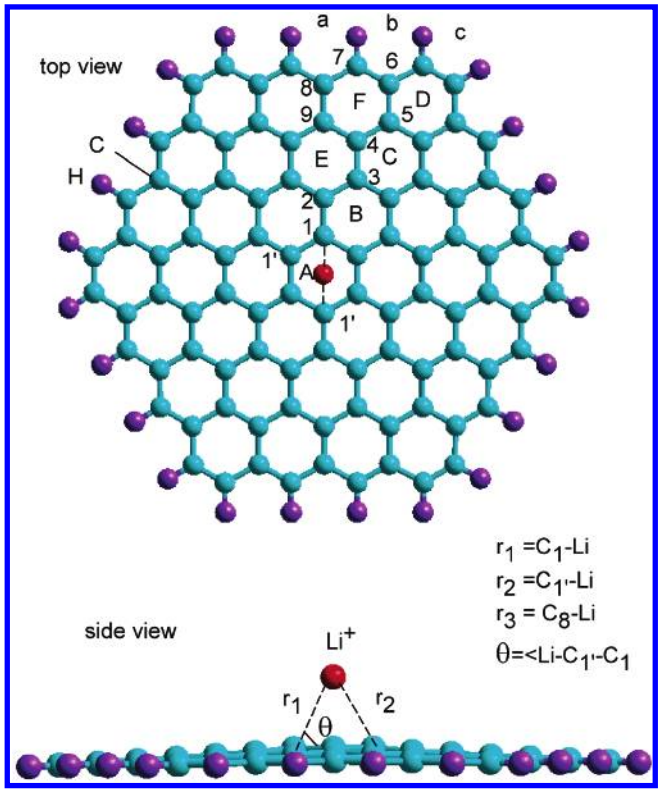

Figure 1. Optimized structures of the $Li^+C_{96}H_{24}$ cluster for site A calculated at the semiempirical AM1 MO level of theory.

TABLE 1: Relative Energies (Δ*E*, in kcal/mol) of the Trapping Sites of Li^+ (A−F and a,b Points) with Respect to That of Site A and Charges on the Li^+ Ion at Trapping Sites (the Values Are Calculated at the AM1 and B3LYP/LANL2DZ Levels of Theory)

	AM1		B3LYP/LANL2DZ	
site	Δ*E*	charge	Δ*E*	charge
A	0.0	+0.734	0.0	+0.788
B	+0.6	+0.731	−0.4	+0.787
C	+0.3	+0.727	−0.7	+0.782
D	−5.9	+0.705	−2.9	+0.720
E	0.0	+0.731	−0.1	+0.785
F	−3.7	+0.715	−3.8	+0.741
a	−3.7	+0.715		
b	−8.4	+0.708		

TABLE 2: Relative Energies (Δ*E*, in kcal/mol) and Charges of the Li^+ Ion Located in Each Point on the Cluster (the Zero Level of the Energy Corresponds to That of Site A, and the Values Are Calculated at the AM1 Level of Theory)

site	Δ*E*	charge	site	Δ*E*	charge
C1	7.22	+0.721	C1−C1″	+4.0	+0.755
C2	4.6	+0.757	C1−C2	+4.5	+0.757
C3	+4.1	+0.757	C2−C3	+3.4	+0.763
C4	+4.3	+0.753	C3−C4	+4.7	+0.743
C5	+9.6	+0.703	C4−C5	+3.2	+0.763
C6	−0.2	+0.734	C5−C6	+4.1	+0.711
C7	−3.3	+0.735	C4−C9	+3.1	+0.768
C8	+3.7	+0.702	C8−C9	+2.9	+0.738
C9	+3.3	+0.770			

found. The charges on Li^+ are dependent on the strapping sites, and the values are changed in the range from +0.705 to +0.734. This result also indicates that about 30% of the electrons of Li^+ are transferred into the carbon surface in all sites. The relative energies and charges on the Li^+ ion for the selected points are given in Table 2. The charges on the Li^+ ion are varied in the range from +0.702 to +0.770. The positions of

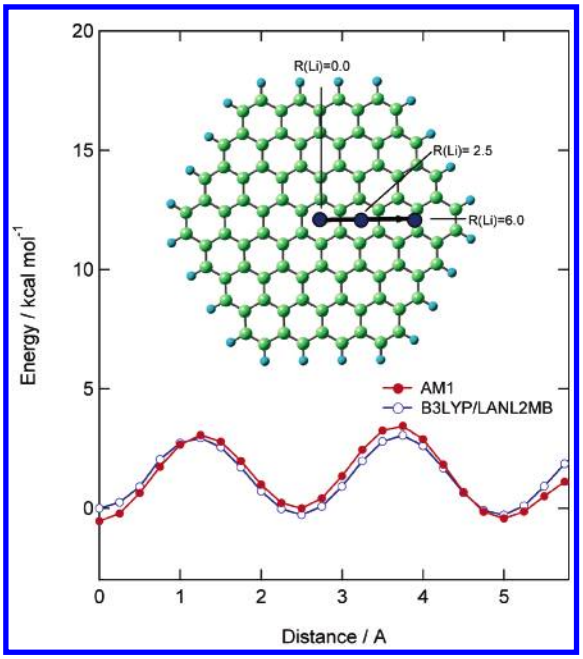

Figure 2. Potential energy curves along the diffusion path of Li^+ on the model cluster $C_{96}H_{24}$. Filled and open circles are calculated by means of the B3LYP/LANL2MB and AM1 methods, respectively. The cluster model and diffusion path are illustrated in the inset.

the Li^+ ion on carbon atoms (C_n, $n = 1-9$) are more unstable in energy except for C_6 and C_7 than site A. All C−C bond positions are also unstable.

Similar calculations for trapping sites (A−F) are carried out at the B3LYP/LANL2DZ level. The results are given in Table 1. As shown in the table, the charges of Li^+ and the relative energies are in reasonable agreement with those obtained by the AM1 calculations. This result indicates that the direct AM1 dynamics would give a reasonable feature for the electronic states of the $Li^+C_{96}H_{24}$ system.

The potential energy curves (PECs) along a typical diffusion path are calculated by means of the AM1 and B3LYP/LANL2MB methods in order to check the level of theory used in the direct MO dynamics calculation. The diffusion path is illustrated in Figure 2 (upper). The dot in the central position represents the Li^+ ion located at the center of mass of the cluster (site A). The arrow indicates the diffusion path assumed in the present calculation. The distance between Li^+ and the surface of the cluster is fixed to 2.24 Å, which is the equilibrium distance of Li^+ on the model cluster. Note that this distance is also close to the equilibrium distance calculated at the B3LYP/LANL2MB level (2.15 Å). The symmetry of the system was kept to C_s during the movement of Li^+ on the surface.

PECs calculated along the diffusion path are plotted in Figure 2. A total of 24 points are calculated from $R(\mathrm{Li}) = 0$ (center) to 5.8 Å. Sites A, B, and C correspond to $R = 0.0$, 2.5, and 5.0 Å, respectively. The PEC calculated by AM1 is in good agreement with that of the DFT calculation. The activation barriers are located in the middle of both sites. Thus, the AM1 calculation well represents the PEC of the DFT calculation. Therefore, we used the direct AM1 dynamics calculation in the present study.

B. Diffusion of Li^+ at Low Temperatures (100−300 K). First, the trajectory calculations are carried out at a lower temperature below 200 K. However, the Li^+ ion does not move and it vibrates around its equilibrium point. The diffusion of Li^+ is found at 250 K. The trajectory of the Li^+ ion at 250 K is illustrated in Figure 3 on the model cluster. At time zero, the

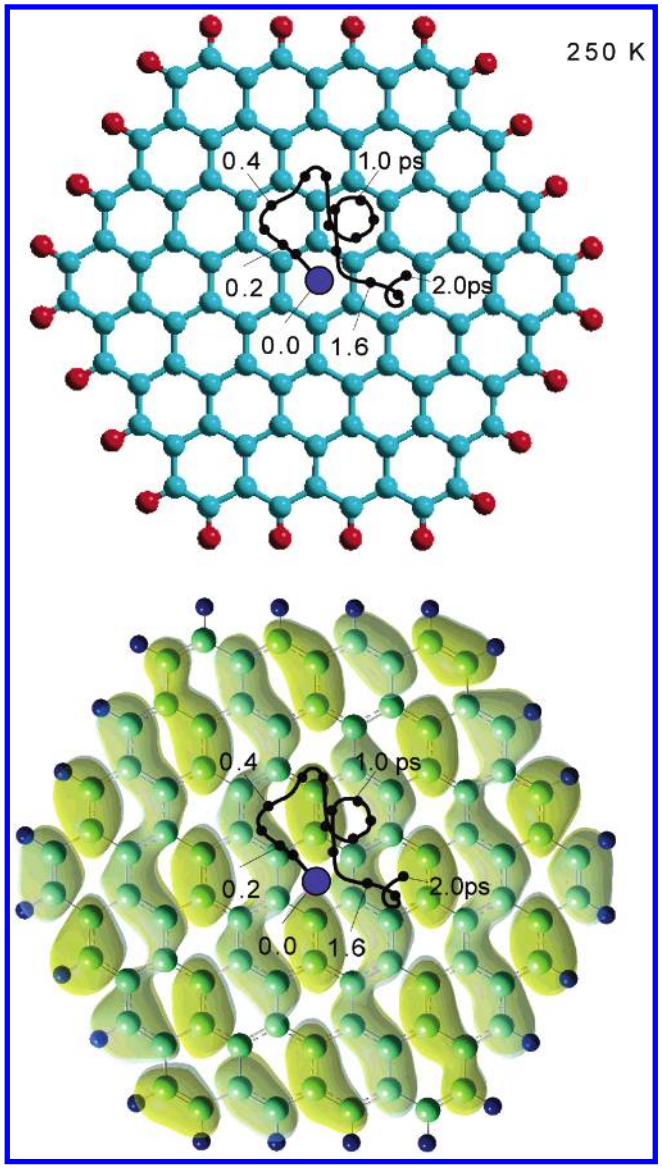

Figure 3. Results of the direct MO dynamics calculation for the diffusion of Li^+ on the $C_{96}H_{24}$ model cluster at 250 K: (upper) trajectory of the Li^+ ion superimposed on the cluster; (lower) HOMO of the model cluster.

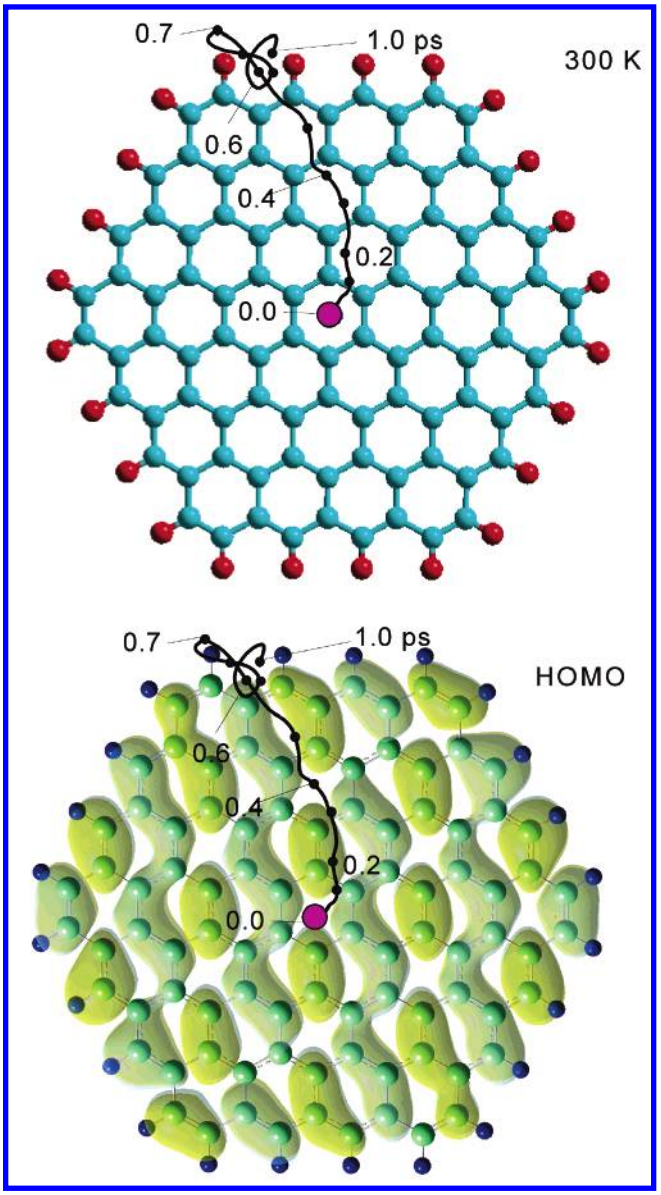

Figure 4. Results of the direct MO dynamics calculation for the diffusion of Li^+ on the $C_{96}H_{24}$ model cluster at 300 K: (upper) trajectory of the Li^+ ion superimposed on the cluster; (lower) HOMO of the model cluster.

Li^+ ion is located in site A and it moves gradually from site A by thermal activation. The Li^+ ion passes near the C_1 carbon at time 0.15 ps, and then, it enters into site B at 0.30 ps. The Li^+ ion moves along the C−C bond, and it reaches the next site (site B) at 0.70 ps.

The trajectory of Li^+ at 300 K is illustrated in Figure 4 as being superimposed on the original plane. The Li^+ ion, started from site A, moves rapidly for the edge of the carbon cluster and reaches the edge at 0.6 ps. The diffusion path from site A to the edge of the cluster is expressed by

$$\text{site A} \rightarrow \text{B} \rightarrow \text{E} \rightarrow \text{F} \rightarrow \text{site b}$$

After that, the Li^+ ion vibrates in the pocket of site b. The Li^+ ion cannot escape from the edge site at 300 K.

The highest occupied molecular orbital (HOMO) of the $Li^+C_{96}H_{24}$ cluster model is plotted as an isosurface in Figure 4. By comparing the diffusion paths with the HOMO, it is found that the Li^+ ion diffuses along a node of the HOMO. This is due to the fact that the 2p orbital of Li^+ interacts strongly with the HOMO during the diffusion process. As will be shown in the next section, the trajectory passes along the node of the HOMO at all temperatures.

Snapshots for 300 K are given in Figure 5. At time zero, the ion is located in site A. After the thermal activation, the ion moves to the edge region. The model cluster is gradually deformed from the flat plane, but the ion still remains in the edge site.

C. Diffusion of Li^+ at 600 K. The trajectory of Li^+ at 600 K is illustrated in Figure 6. The Li^+ ion, started from site A, runs rapidly against the edge of the carbon cluster and reaches the edge at 0.4 ps. After that, the ion moves again on the carbon plane in the range 0.4−1.0 ps.

The diffusion path for 600 K is expressed by

$$\text{site A} \rightarrow \text{B} \rightarrow \text{E} \rightarrow \text{F} \rightarrow \text{site a} \rightarrow \text{site b} \rightarrow \text{F} \rightarrow \text{E} \rightarrow \text{B} \rightarrow \text{A}$$

Snapshots are given in Figure 7. At time zero, the ion is located in site A. After the thermal activation, the ion moves to the edge region. At 0.4 ps, the ion reaches the edge region.

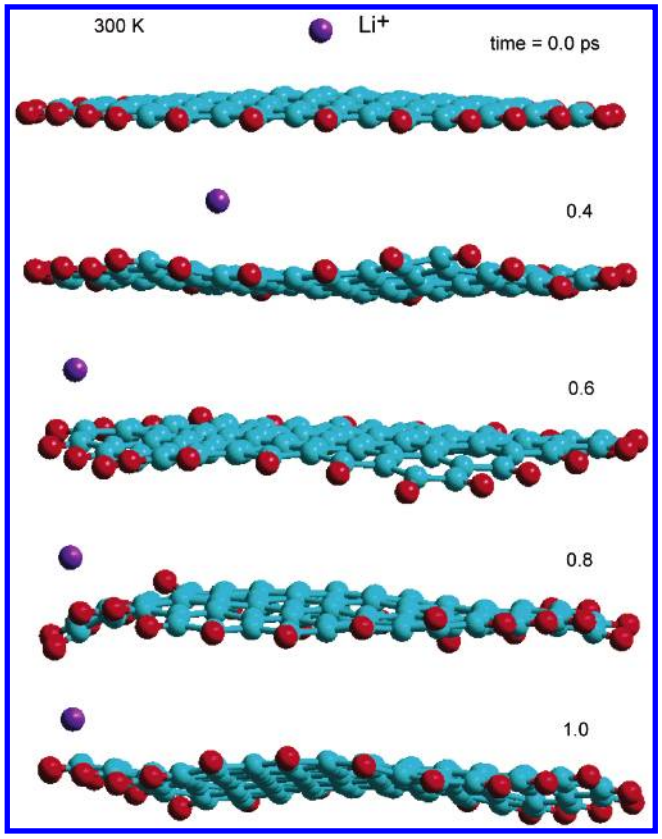

Figure 5. Snapshots of the $Li^+C_{96}H_{24}$ system at 300 K.

After that, the ion moves under the surface. Similar trajectories are obtained for higher temperatures.

D. Diffusion Coefficients. In this section, the diffusion coefficients of Li^+ are calculated for all temperatures. The diffusion coefficients of Li^+ are calculated using the time-dependent square displacement (TSD), which is expressed by

$$\mathrm{TSD} = R^2 \equiv \sum_{i=1}^{M} (r_i(t + \Delta t) - r_{i-1}(t))^2 \qquad (3)$$

where M is the total number of steps in the trajectory calculation and r_i is the position of Li^+ at the ith step. In Figure 8, the TSD data for 250−1000 K are plotted as a function of time. The Li^+ ion did not diffuse below 250 K. As shown in Figure 8, the TSD increases gradually with increasing simulation time. The slope of the lines becomes larger at higher temperatures.

Next, we assume that the diffusion coefficient (D) is expressed by the following relationship:

$$R^2 = 6Dt + B \qquad (4)$$

where B is the small thermal factor arising from atomic vibration which is negligibly small in the present calculation. The calculated diffusion coefficients at simulation temperatures of 800−1100 K are plotted in Figure 9. The diffusion coefficients for 250, 500, and 1000 K are calculated to be 0.25×10^{-10}, 1.98×10^{-10}, and 7.60×10^{-10} m^2/s, respectively.

The diffusion coefficients are also calculated using the mean square displacement (MSD)[30,31]

$$\langle r_i^2(t) \rangle = \frac{1}{N} \sum_{i=1}^{N} [r_i(t) - r_i(t = 0)]^2 \qquad (5)$$

where N is the total number of ions in the system and $r_i(t)$ is the position of ion i at time t. This is an usual method for obtaining the diffusion coefficient in the case of long range and long time MD simulation. The diffusion coefficients calculated using the MSD are given in Figure 9. The coefficient increases with increasing temperature, which is in qualitative agreement with the result of the TSD. However, the magnitude of D calculated using the MSD is larger than that calculated using the TSD. The coefficient at 1000 K is calculated to be 4.7×10^{-8} m^2/s, which is significantly larger than the experimental value (1.9×10^{-10} m^2/s at 1000 K) and that obtained by the TSD (7.6×10^{-10} m^2/s at 1000 K). This difference is due to the fact that the time period is very short in the present case.

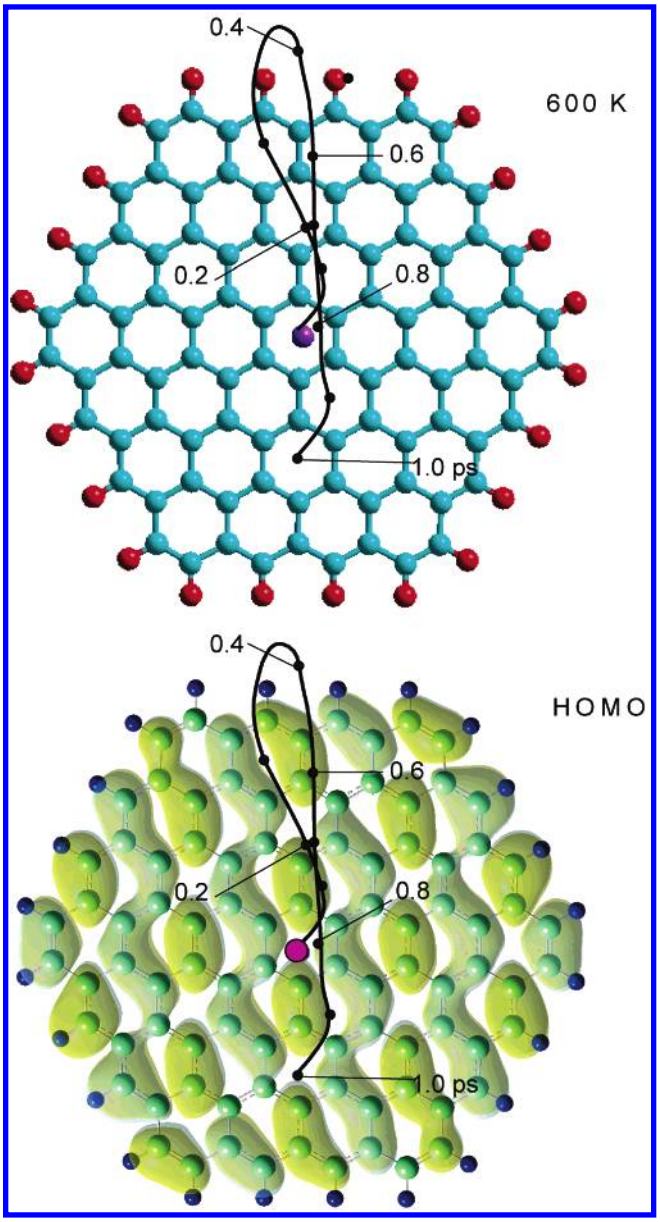

Figure 6. Results of the direct dynamics MO calculation for the diffusion of Li^+ on the $C_{96}H_{24}$ model cluster at 600 K: (upper) trajectory of the Li^+ ion superimposed on the cluster; (lower) HOMO of the model cluster.

4. Discussion

A. Diffusion Path of Li^+ on the Carbon Cluster Model. In the present study, the diffusion processes of Li^+ on the model cluster are investigated by means of the direct MO dynamics method. The dynamics calculations indicate clearly that the

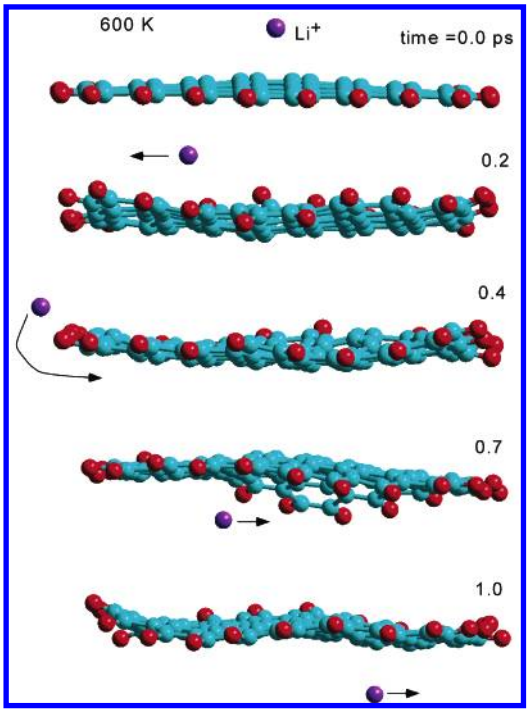

Figure 7. Snapshots of the $Li^+C_{96}H_{24}$ system at 600 K.

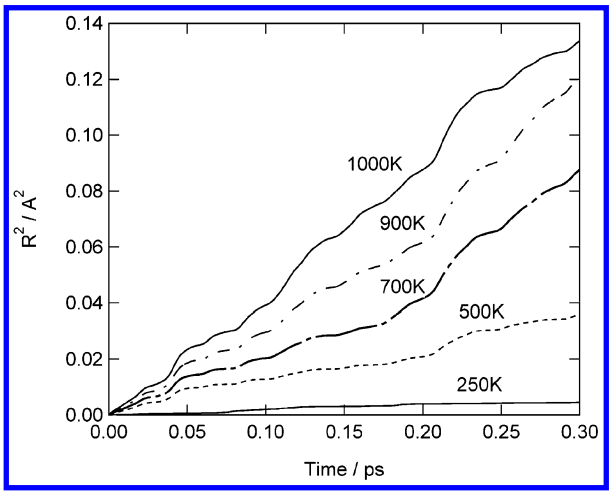

Figure 8. Time-dependent square displacement (TSD) of the Li^+ ion on the $C_{96}H_{24}$ carbon cluster, calculated in the temperature range 250−1000 K.

diffusion of the Li^+ ion proceeds along the node of the HOMO of the carbon cluster. This is due to the fact that the 2p orbital of Li^+ is parallel to the molecular plane of the carbon cluster and interacts with the HOMO of the cluster during the diffusion. Therefore, the diffusion path is restricted. This feature is only obtained by the direct MO dynamics method.

Next, let us consider the temperature effect on the diffusion processes of Li^+. We calculated the dynamics at nine temperatures from 200 to 1000 K. The calculations indicated that diffusion of Li^+ did not occur below 200 K because there is an activation barrier to transfer from site A. Above 250 K, the Li^+ ion moves on the surface of the carbon cluster, but the region of the diffusion is narrow. At 600−800 K, the Li^+ ion can move freely on both the bulk surface and the edge regions. At higher temperatures, the Li^+ ion can run and escape from the plane.

A model of the diffusion process of Li^+ on the amorphous carbon is illustrated in Figure 11. At lower temperatures (below 200 K), the surface of the carbon cluster is hardly vibrated, the Li^+ ion vibrates around the equilibrium point. At intermediate

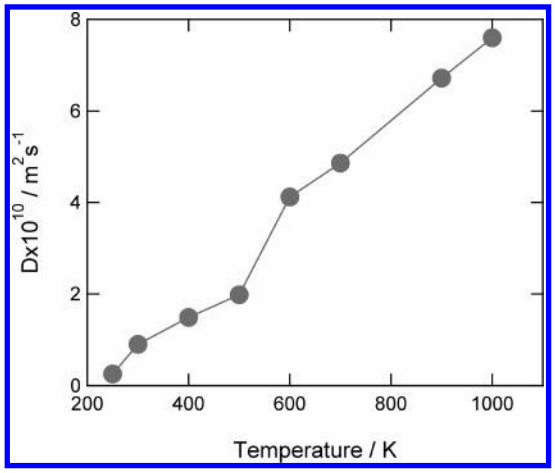

Figure 9. Diffusion coefficients (D) of the Li^+ ion on the $C_{96}H_{24}$ cluster calculated with the TSD obtained by direct MO dynamics calculations at the AM1 level.

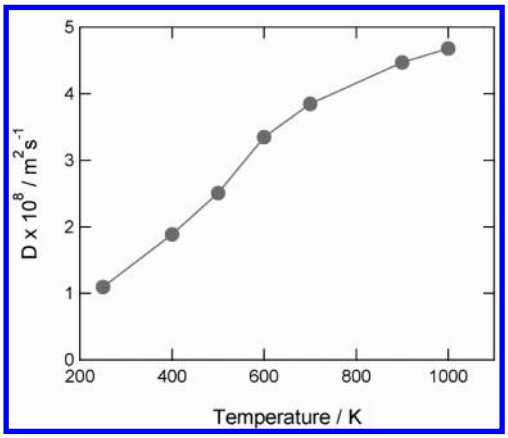

Figure 10. Diffusion coefficients (D) of the Li^+ ion on the $C_{96}H_{24}$ cluster calculated with the MSD obtained by direct MO dynamics calculations at the AM1 level.

temperatures (about 250 K < T < 400 K), the Li^+ ion moves on the carbon surface and it falls in the edge region and still remains in the edge region. The ion moves freely on both the surface and edge regions at 800−1000 K. Thus, the Li^+ ion transport process on the model cluster is strongly dependent on temperature.

B. Diffusion Coefficients of Li^+. In the present work, we calculated the diffusion coefficients at the AM1 dynamics level. The diffusion coefficient of Li^+ in the model cluster is calculated to be 0.90×10^{-10} m^2/s at room temperature (300 K). The coefficients increase linearly with increasing temperature. At 1000 K, the coefficient is calculated to be 7.60×10^{-10} m^2/s. Jungblut and Hoinkis estimated experimentally the diffusion coefficient as a bulk diffusion process to be 7.60×10^{-10} m^2/s at 1070 K and 1.90×10^{-10} m^2/s at 1000 K.[22] Thus, the present calculated value at 1000 K is 4 times faster than that of experiment. This difference may be due to the fact that the activation barrier is slightly underestimated in the AM1 and B3LYP/LANL2MB calculations. A more accurate wave function would give a more realistic diffusion process.

C. Comparison with Previous Studies. The static properties for the interactions between the lithium ion (atom) and carbon clusters have been investigated theoretically by several groups.[14−18,27] The binding energy of Li^+/Li on each trapping site was investigated by means of semiempirical MO calculations. These calculations showed that the Li^+ ion is more stabilized at the edge site than at the surface bulk site.[15,27b,28]

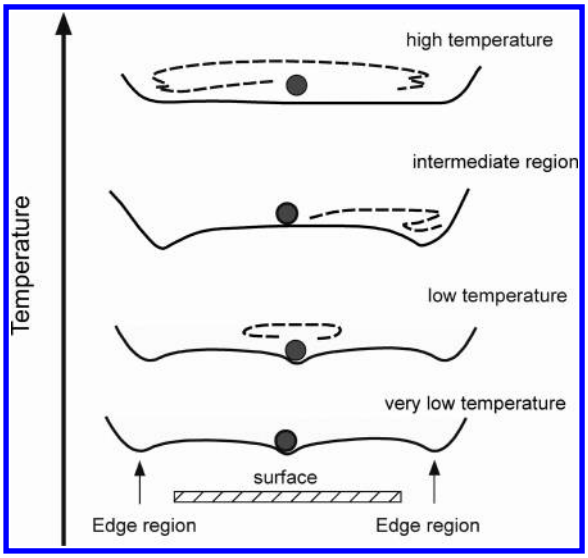

Figure 11. Model for the diffusion of Li^+ on an amorphous carbon surface (very lower temperature below 200 K): the Li^+ ion still remains in the center of mass of the carbon cluster: (low temperature) the Li^+ ion vibrates around the equilibrium point (site A); (intermediate region) the Li^+ ion moves easily on the surface and the edge region of the cluster; (high temperature) the Li^+ ion moves freely on the surface and the edge region.

These results are in good agreement with the results of the present static MO calculations.

Panapek et al.[27b] investigated the interaction between Li^+ ions and a disordered carbon−hydrogen alloy (amorphous carbon) by means of semiempirical MNDO and AM1 methods using the $C_{54}H_{18}$ model cluster. They showed that large amounts of Li ions can be adsorbed to the surfaces. In particular, Li^+ was preferentially bound to the hydrogen terminated edges of hexagonal carbon fragments.

Hankinson and Almlöf carried out a pioneering calculation for the interaction of the Li atom with a carbon layer using ab initio MO calculations.[18] They showed that the Li atom interacting with the carbon layer exists as a positive ion and the minimum energy path from site A to the circumference region (site b) is A → B → C → b (see Figure 1), which is analogous to the present calculations for the Li^+ ion.

In previous papers, we investigated the diffusion dynamics of the Li^+ ion on a small-sized carbon cluster ($C_{54}H_{18}$) using direct MO dynamics calculations.[32,33] At 800 K, the ion is transferred freely on surface and edge regions. This feature is similar to the present results.

D. Concluding Remarks. In the present study, we have introduced several approximations to calculate the potential energy surface and to treat the diffusion dynamics. First, we assumed that amorphous carbon is composed of a $C_{96}H_{24}$ carbon model cluster. X-ray diffraction revealed the presence of few-layer graphitic fragments of order 40 lateral dimension corresponding to ∼20 contiguous hexagons.[34] The model cluster used in the present study has 37 hexagons. Also, the amorphous carbon does not have a stacked layer structure.[25,26] Therefore, the model cluster used in the present study would be enough to represent the structure of actual amorphous carbon. However, to obtain more accurate information on the diffusion process on amorphous carbons, dynamics calculations using several sizes of cluster models would be required.

Also, we assumed the AM1 multidimensional potential energy surface in the trajectory calculations throughout. This level of theory would be adequate to discuss qualitatively the diffusion dynamics of Li^+. In particular, the AM1 calculation well represents the barrier height and shape of the potential energy curve along the diffusion path of Li^+ calculated by a more sophisticated level (B3LYP/LANL2MB), as shown in Figure 2. Hence, the direct MO dynamics calculations at this level of theory would give a reasonable feature on the diffusion process of Li^+ on the carbon cluster. However, more accurate wave functions may provide deeper insight into the detailed diffusion dynamics. Despite the several assumptions introduced here, the results enable us to obtain valuable information on the mechanism of diffusion of the Li^+ ion on an amorphous carbon cluster.

Acknowledgment. The authors are indebted to the Computer Center at the Institute for Molecular Science (IMS) for the use of the computing facilities. One of the authors (H.T.) also acknowledges partial support from a Grant-in-Aid for Scientific Research (C) from the Japan Society for the Promotion of Science (JSPS).

Supporting Information Available: Figures showing the time evolution of total energy and the effects of temperature and initial conditions on the Li^+ diffusion dynamics. This material is available free of charge via the Internet at http://pubs.acs.org.

References and Notes

(1) Inagaki, M. In *Chemical Physics of Intercalation*; Legrand, A. P., Flandrois, S., Eds.; NATO ASI Series B, 172; Plenum: New York, 1987; p 105.
(2) For a review article, see: Inagaki, M. *J. Mater. Res.* **1989**, *4*, 1560.
(3) For a review article, see: Koksbang, R.; Barker, J.; Shi, H.; Saidi, M. Y. *Solid State Ionics* **1996**, *84*, 1.
(4) Inagaki, M.; Tachikawa, H.; Nakahashi, T.; Konno, H.; Hishiyama, Y. *Carbon* **1998**, *36*, 1021.
(5) Konno, H.; Oka, H.; Shiba, K.; Tachikawa, H.; Inagaki, M. *Carbon* **1999**, *37*, 887.
(6) Shimizu, A.; Inagaki, M.; Tachikawa, H. *J. Phys. Chem. Solids* **1999**, *60*, 1811.
(7) Konno, H.; Shiba, K.; Tachikawa, H.; Nakahashi, T.; Oka, H.; Inagaki, M. *Synth. Met.* **2001**, *125*, 189.
(8) Guerard, D.; Herold, A. *Carbon* **1975**, *13*, 337.
(9) Yata, S.; Hato, Y.; Kinoshita, H.; Ando, N.; Anekawa, A.; Hashimoto, T.; Yamaguchi, M.; Tanaka, K.; Yamabe, T. *Synth. Met.* **1995**, *73*, 273.
(10) Tachikawa, H. *J. Phys. Chem. A* **2004**, *108*, 7853.
(11) Tachikawa, H. *Chem. Phys. Lett.* **2003**, *370*, 188.
(12) Tachikawa, H.; Kawabata, H. *J. Phys. Chem. B* **2003**, *107*, 1113.
(13) Tachikawa, H. *J. Phys. Chem. A* **2002**, *106*, 6915.
(14) Marquez, A.; Vargas, A.; Balbuena, P. B. *J. Electrochem. Soc.* **1998**, *145*, 3328.
(15) Nakadaira, M.; Saito, R.; Kimura, T.; Dresselhaus, G.; Dresselhaus, M. S. *J. Mater. Res.* **1997**, *12*, 1367.
(16) Fujita, M.; Wakabayashi, K.; Nakada, K.; Kusakabe, K. *J. Phys. Soc. Jpn.* **1996**, *65*, 1920.
(17) Boehm, R. C.; Banerjee, A. *J. Chem. Phys.* **1992**, *96*, 1150.
(18) Hankinson, D. J.; Almlöf, J. *THEOCHEM* **1996**, *388*, 245.
(19)] Lunell, S.; Stashans, A.; Ojamae, L.; Lindstrom, H.; Hagfeldt, A. *J. Am. Chem. Soc.* **1997**, *119*, 7374.
(20) Ishikawa, S.; Madjarova, G.; Yamaba, T. *J. Phys. Chem. B* **2001**, *105*, 11986.
(21) Suzuki, T.; Hasegawa, T.; Mukai, S. R.; Ta'om, H. *Carbon* **2003**, *41*, 1933.
(22) Jungblut, B.; Hoinkis, E. *Phys. Rev. B* **1989**, *40*, 10810.
(23) Armstrong, A. R.; Bruce, P. G. *Nature* **1996**, *381*, 499.
(24) Sato, K.; Noguchi, M.; Demachi, A.; Oki, N.; Endo, M. *Science* **1994**, *264*, 556.
(25) Houska, C. R.; Warren, B. E. *J. Appl. Phys.* **1954**, *25*, L503.
(26) Dahn, J. R.; Zheng, T.; Yinghu, L.; Xue, J. S. *Science* **1995**, *270*, 590.
(27) (a) Ago, H.; Nagata, K.; Yoshizawa, K.; Tanaka, K.; Yamabe, T. *Bull. Chem. Soc. Jpn.* **1997**, *70*, 1717. (b) Papanek, P.; Radosavljevic, M.; Fischer, J. E. *Chem. Mater.* **1996**, *8*, 1519.
(28) Berendsen, H. J. C.; Postma, J. P. M.; van Gunsteren, W. F.; di Nola, A.; Haak, J. R. *J. Chem. Phys.* **1984**, *81*, 3684.

(29) Ab initio MO calculation program: Frisch, M. J.; Trucks, G. W.; Schlegel, H. B.; Scuseria, G. E.; Robb, M. A.; Cheeseman, J. R.; Montgomery, J. A., Jr.; Vreven, T.; Kudin, K. N.; Burant, J. C.; Millam, J. M.; Iyengar, S. S.; Tomasi, J.; Barone, V.; Mennucci, B.; Cossi, M.; Scalmani, G.; Rega, N.; Petersson, G. A.; Nakatsuji, H.; Hada, M.; Ehara, M.; Toyota, K.; Fukuda, R.; Hasegawa, J.; Ishida, M.; Nakajima, T.; Honda, Y.; Kitao, O.; Nakai, H.; Klene, M.; Li, X.; Knox, J. E.; Hratchian, H. P.; Cross, J. B.; Bakken, V.; Adamo, C.; Jaramillo, J.; Gomperts, R.; Stratmann, R. E.; Yazyev, O.; Austin, A. J.; Cammi, R.; Pomelli, C.; Ochterski, J. W.; Ayala, P. Y.; Morokuma, K.; Voth, G. A.; Salvador, P.; Dannenberg, J. J.; Zakrzewski, V. G.; Dapprich, S.; Daniels, A. D.; Strain, M. C.; Farkas, O.; Malick, D. K.; Rabuck, A. D.; Raghavachari, K.; Foresman, J. B.; Ortiz, J. V.; Cui, Q.; Baboul, A. G.; Clifford, S.; Cioslowski, J.; Stefanov, B. B.; Liu, G.; Liashenko, A.; Piskorz, P.; Komaromi, I.; Martin, R. L.; Fox, D. J.; Keith, T.; Al-Laham, M. A.; Peng, C. Y.; Nanayakkara, A.; Challacombe, M.; Gill, P. M. W.; Johnson, B.; Chen, W.; Wong, M. W.; Gonzalez, C.; Pople, J. A. *Gaussian 03*, revision B.04; Gaussian, Inc.: Pittsburgh, PA, 2003.

(30) Fisher, C. A. J.; Matsubara, H. *Comput. Mater. Sci*. **1999**, *14*, 177.

(31) Khan, M. S.; Islam, M. S.; Bates, D. R. *J. Mater. Chem*. **1998**, *8*, 2299.

(32) Shimizu, A.; Tachikawa, H. *Chem. Phys. Lett.* **2001**, *339*, 110.

(33) Shimizu, A.; Tachikawa, H. *THEOCHEM* **2001**, *544*, 173.

(34) Liu, Y.; Xue, J. S.; Zheng, T.; Dahn, J. R. *Carbon* **1996**, *34*, 193.